

# Experimental and numerical study of natural ventilation in four-sided wind tower traps

## Authors

Davoud Jafari<sup>a</sup>  
Alireza Shateri<sup>a\*</sup>  
Afshin Ahmadi Nadooshan<sup>a</sup>

<sup>a</sup> Faculty of Engineering, Shahrekord University, Shahrekord, Iran

## ABSTRACT

*In the past, wind towers were applied as the main architectural part of building construction in the desert areas of Iran. These almost high structures were used as cooling load suppliers at residential buildings. In the present study, the effect of symmetric four-sided wind tower in flow induction to the bottom space has been analysed by using a wind tunnel and numerical simulations. In the numerical simulation, the flow is assumed to be three-dimensional, unsteady, compressible and turbulent. The experimental studies have been performed by placing a model of these structures at a laboratory wind tunnel. At this state, crossing airflow through every channel is measured for analysing the induction performance of wind tower at different angles of wind blowing. Moreover, the turbulence effect is analysed by adding horizontal and vertical blades and crowns at the top and bottom of the internal gate of traps for attaining better performance. Two different geometries are used for simulations. The results showed that inserting the blade and crown at the bottom and top affect on the flow rate have effect on the flow rate. For instance, inserting horizontal blades and crown at the top of the model leads to 8 and 16% increase in the flow rate, respectively. The results of the numerical simulations have shown acceptable agreement with experimental results.*

## Article history:

Received : 7 November 2017  
Accepted : 9 December 2017

**Keywords:** Wind Tower, Wind Tunnel, Natural Ventilation, Numerical Simulation.

## 1. Introduction

Nowadays, natural ventilation is widely used in modern buildings. The main purposes of using natural ventilation are to reduce energy consumption as well as to minimize the spread

of dangerous gases to the environment. Wind towers have been used in Iran and areas adjacent to the Persian Gulf over the past centuries [1-3]. The shape, height and internal structure of wind towers, especially in desert areas, besides cooling load supply, reflect the culture and potentials of Iranian architecture [4, 5]. Wind towers supply the whole or part of the required

\* Corresponding author: Alireza Shateri  
Faculty of Engineering, Shahrekord University,  
Shahrekord, Iran  
Email: shateri@eng.sku.ac.ir

ventilation at residential buildings without using current mechanisms. Figure 1 shows a view of an applied four-sided wind tower in Yazd city of Iran. These days, in many countries like England and some other European nations, wind towers are extendedly used in residential buildings [6]. Wind flow on a wind tower causes noticeable pressure difference around the wind towers, which cause airflow induction to the internal place of residential areas. Air enters from the wind tower traps with positive pressure coefficient and exits from the external traps with negative pressure coefficient [7]. If in a definite area, wind blowing mostly occurs in a special direction (dominant wind); this structure would be able to have one internal trap in that direction and another one in the opposite direction for absorbing external airflow. Otherwise, wind towers usually have several traps in order to guide part of wind blowing to residential internal space [8, 9]. The use of several-sided wind towers was common in Iran. Wind towers with a height of 5 to 33 m are installed on the ceiling of buildings. In taller wind towers, the wind velocity is higher and a lower amount of dust enters the building [7].

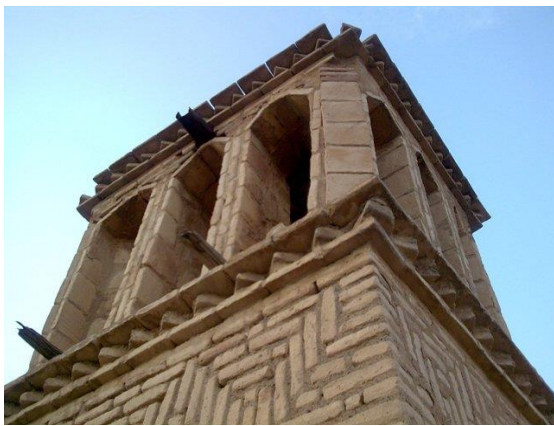


Fig. 1. Four-sided wind tower in the city of Yazd.

The number of wind tower traps is different. Wind towers are often classified on the basis of trap numbers. The different kinds of wind towers are: 1-sided, 2-sided, 4-sided and 6-sided. One of the old buildings to use wind towers is Dowlatabad garden, which is located in Yard Province [10]. In new designs, the wind towers are constructed of two or four compositions. Wind could flow through the designed channels separately to the bottom, and if wind blows in every direction, it would be able to enter the building through wind tower traps [11, 12]. In his study, Bahadori [13] tested a wind tower's pressure coefficient

at a house and its yard with the scale of 1:100 in which wind was simulated via several vertical curtains. In addition, the effect of neighbouring homes on the pressure coefficient was analysed. Karakatsanis et al. [14] studied Bahadori's model [13]. In their research, they applied prototype building using several scales and analysed the boundary layer effect in the wind tunnel. Elmualim and Hazim [15] have performed numerical and laboratory research on the performance of square wind tower. They explained this was due to the fact that the sharp edges of the square create a large region of flow separation and higher pressure difference across the device. The hydrodynamic analysis of flow in wind towers was done by Montazeri and Dehghan [16] using CFD technique. That work was based on the numerical solution of the two-dimensional Navier–Stokes. They concluded that the separated flow and wake region near the lower edge of the wind tower opening considerably decreased the induced capacity of the wind tower. Elmualim [17] analysed a wind tower performance at a real laboratory.

The results showed that basically, the ventilation rate in the chosen design (closed window room) was more than the opened window room. In their laboratory research, Montazeri et al. [18] analysed a one-sided wind tower. This research evaluated the induced flow rate to the wind tower (or its external flow) and the pressure coefficient on various surfaces. The results revealed that one-direction wind towers show suitable performance in whole blowing directions. Elmualim [19] simulated a wind tower that consisted of a damper and a heat source and its ability was evaluated, and the analysis showed that there was a relative conformity between numerical simulation and laboratory results. Montazeri [20] analysed 5 cylindrical wind tower types and compared them with previous studies. Montazeri evaluated the performance of 1-directional model at places where the dominant wind was blowing from a one-sided well. As we know, experimental methods are often more expensive than numerical methods, and due to simplification of the dominant equations on fluid flow and the errors of turbulent model or boundary condition, it would affect the accuracy of results. It is better to compare accurate results with experimental results and design the best model.

The present study evaluated the condition circumstance of air induction to the wind

directional traps, lateral traps, and traps that are located opposite the wind direction and a variety of air flow rate suction and blow with different angles considering numerical and laboratory methods, and the results were compared. Moreover, the wind tower performance, as a ventilation device, through suitable air suction was analysed. Then, the turbulence effect on the internal traps of wind towers was evaluated.

## 2. Experimental Methodology

Experiments were performed at Azad University, Majlesi branch. The wind tunnel used was a blow and suction tunnel, and had a test section with height, width and length of 60, 60 and 200 cm, respectively. Based on the model and the wind tunnel suction dimensions, 5.5% obstruction was made by the scaled model so that pressure correction was not required.

Figure 2 shows the wind tunnel applied in laboratory tests. In aerodynamic studies, it is essential that the prototype Reynolds number,  $Re = \rho UD/\mu$ , is the same as the main model, where  $D$  is the hydraulic diameter of the entrance of the tunnel.

The scale of 1:40 was the ratio to main model so that the wind velocity should be 40 times greater and it is almost impossible, but hydrodynamics properties around the buildings showed that air flow was independent of the Reynolds number, and if velocity became more than the specified special velocity, the velocity variation would not affect the flow condition [10].

Figure 3 shows the variation of pressure coefficient for different values of the incident angles. The wind pressure coefficient  $C_p$  is defined by the following formula:

$$C_p = \frac{P - P_s}{1/2\rho v^2} \quad (1)$$

In this equation,  $P$  is the flow pressure at various model points, which is measured by set sensors in the model.  $P_s$  is the static pressure, and  $1/2\rho v^2$  is the dynamic pressure. In this graph, the velocity is based on m/s and the wind tower height is calculated on the basis of mm. It is obvious from the figure that at pressure coefficients above 10 m/s, the variation becomes uniform and it is clear that increasing the velocity does not have any influence on the flow regime. Therefore, the tests are performed for  $0^\circ$ - $90^\circ$  angles with  $10^\circ$  steps. All the stages of the test are at uniform condition and wind tunnel velocity is 20 m/s.

### 2.1. The wind tower models

Wind tower models are four-sided and made with wood having length, width and height of 7, 7 and 30 cm, respectively. The internal traps of the prototypes have 4-sides: A, B, C and D with every side using distinct channels for air induction to the bottom space. The bottom of the wind tower and the bottom of the tunnel in a home are located from where inducted air enters and the environmental air doesn't have any effect on air suction from wind towers.



Fig. 2. The wind tunnel and experimental test box.

Model I is a symmetric cylindrical wind tower that consists of 2 blades with 3 mm thickness on 4 quarters and the dimensions of the wind tower internal trap are 3.1cm×6.72cm and the internal channel area is a circle quarter with a radius of 3.5 cm. Model II is also a symmetric triangular section wind tower in which the dimensions of the wind tower internal trap are 6.72 cm×6.4 cm. Figure 4

shows wind tower models with bottom space. The wind towers have been modelled with bottom space and they have been tested in the wind tunnel. The bottom space is a cubic home made of wood and all manes are 34.72 cm. Figure 5 shows the wind tower properties, its bottom space, and the model rotation around the wind tunnel.

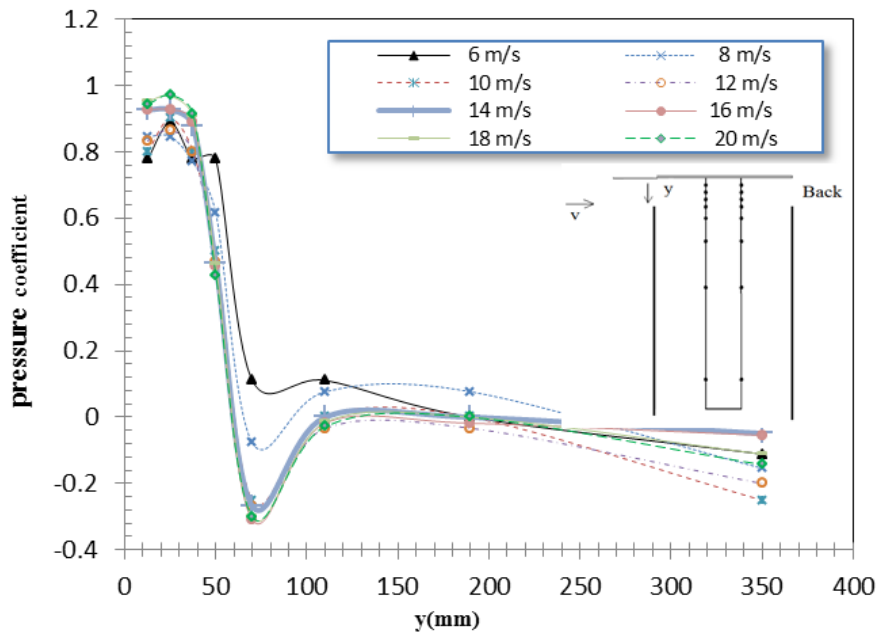


Fig. 3. Variation of the pressure coefficients for different values of the incident air stream velocity.

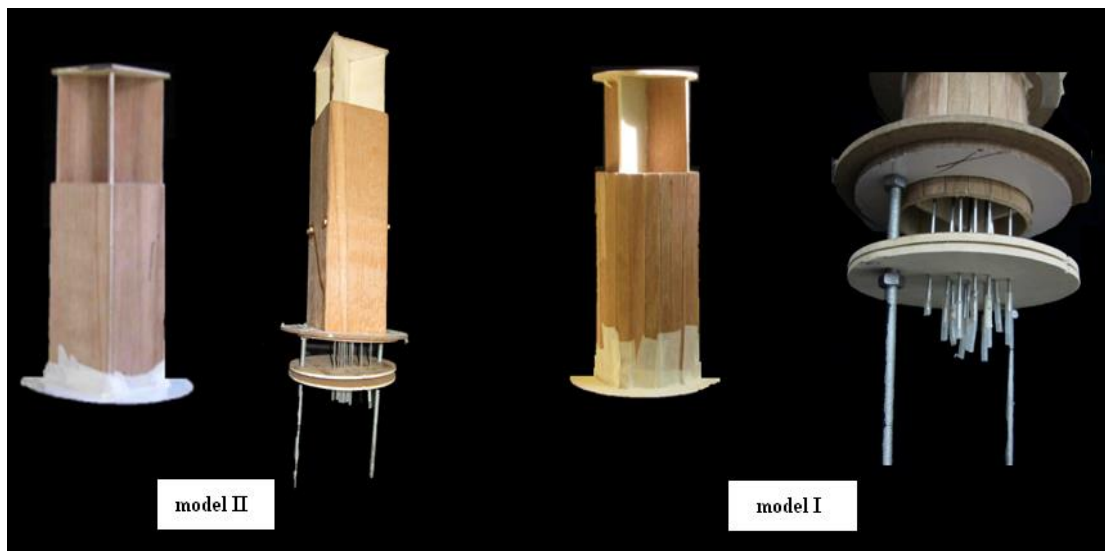


Fig. 4. Four-sided wind tower models with the attached pressure tabs.

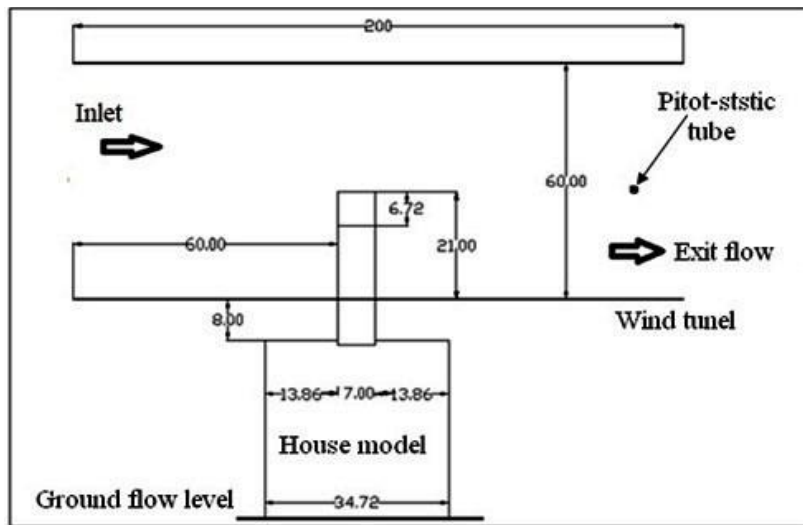


Fig. 5. Location of wind tower and test room in relation to the wind tunnel.

2.2. Measurement procedures


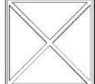
Basically, a pitot tube measures the flow rate and velocity by determining the difference between the total pressure or impact pressure and the static pressure. The difference between the pressures is called dynamic pressure, and it is related to velocity by using the equation derived from Bernoulli's principle. Therefore, it is essential to determine the difference between the static pressure and the total pressure (impact pressure) for calculating the dynamic pressure (kinetic) and the velocity at a certain point of the fluid flow stream. The total pressure is measured by a total pressure tube. The pressure tube is installed in such a way that its trap surface is located parallel to the fluid's stream lines. The static pressure is measured by a static pressure tube. The static and total pressure tubes should be located along the stream lines because the fluid velocity at a certain point is derived from the difference between total and static pressures. The tubes applied in this study were made of steel with an inner diameter of 1 mm and an

outer diameter of 1.2 mm. The other characteristics are illustrated in Fig. 6. One of the advantages of pitot static tubes is low error while the tube axis has got little deviation from the fluid stream line. The angle between the tube axis and the fluid stream lines direction is introduced as 'angle of attack' or 'angle of deviation'. If the angle is low, the total pressure and the static pressure change almost at the same ratio, and the dynamic difference between the two until 16° deviation is nearly constant [16,10,18]. For measuring pressure, some total and pressure tubes were applied. These tubes are shown in Table. 1.

A differential pressure manometer should be installed on the head of the pitot and the static pressure tubes. Therefore, it was decided to use more pitot tubes at the bottom of the windward channel. The cross section area of the channel was divided into several portions. The air flow rate passing through it, is calculated as shown below:

$$Q = \sum A_i V_i \tag{2}$$

Table 1. The number of pitot and static tubes at the bottom and top surfaces of the models.

Wind catcher models	Pitot tube		Static tube		Openings
	Up	Down	Up	Down	
Model I	11	4	11	4	
Model II	11	4	11	4	

where  $Q$  is the flow rate through the channel of wind tower and  $A_i$  and  $V_i$  are the area and velocity of portion  $i$ .

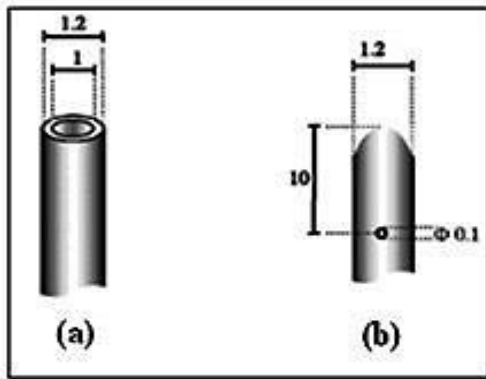


Fig. 6. (a) Pitot tubes and (b) Static tubes.

### 2.3. Natural ventilation efficiency

The natural ventilation efficiency of a 4-sided wind tower model can be measured by Eq.(3).

$$\text{Natural Ventilation Efficiency (\%)} = \frac{Q}{Q_0} \times 100 \quad (3)$$

In this equation,  $Q$  is the internal flow at different angles and  $Q_0$  is the internal flow at  $0^\circ$  angle. This efficiency reveals the angle at which the maximum air suction to the bottom space occurs. Using this parameter, it is possible to analyse wind tower performance at different wind blowing angles [3].

### 2.4. Making turbulence in the wind tower trap

In this section, by inserting vertical blades, horizontal blades and crowns at the top and the bottom of Model II, the turbulence effect on the internal wind tower traps is considered. The status of inserting the blades and crowns is shown in Fig. 7.

### 3. Numerical solution

In the present study, experimental models are simulated numerically using Ansys Fluent software. Three-dimensional governing equations are discretised using finite volume based method and SIMPLEC algorithm. The turbulence  $\kappa$ - $\epsilon$  turbulence approach is used to model the turbulent flow. Conservation of mass equation

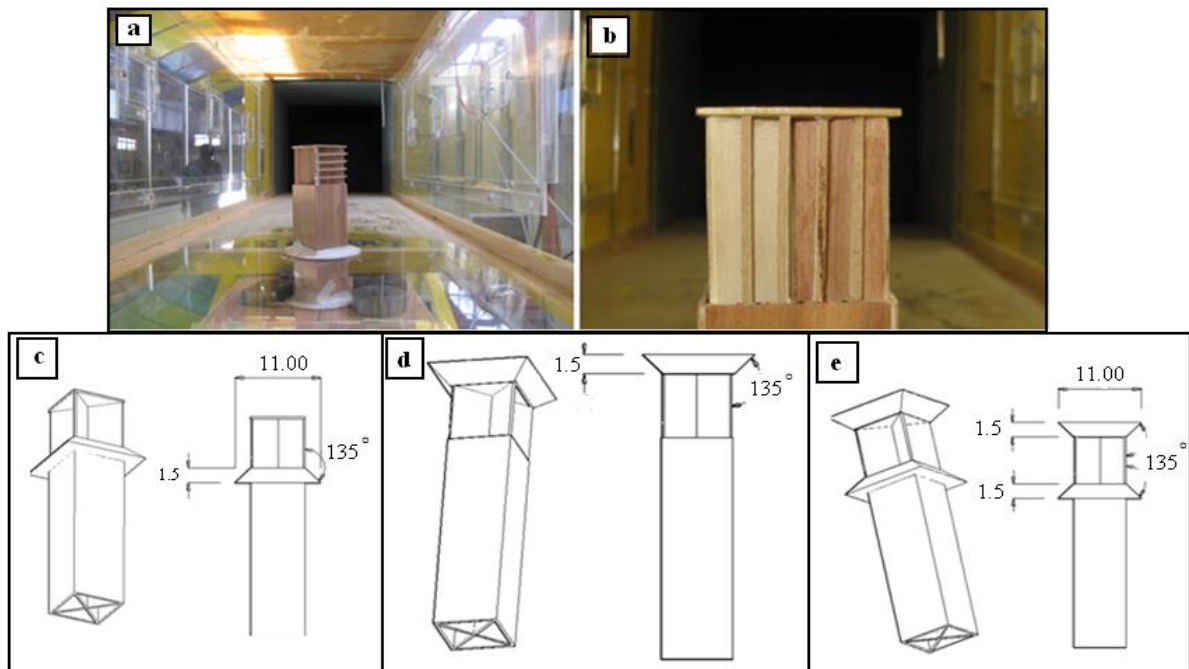


Fig. 7. Inserting mode of (a) vertical blades, (b) horizontal blades, (c) crowns at the top, (d) crowns at the bottom, and (e) crowns at the top and the bottom.

$$\frac{\partial(\rho u_i)}{\partial x_i} = 0 \quad (4)$$

where  $u_i$  and  $\rho$  are the fluid velocity term in the  $x$  direction and the air density.

Momentum equations:

$$\rho u_j \frac{\partial u_i}{\partial x_j} = \frac{\partial p}{\partial x_i} + \frac{\partial}{\partial x_j} \left[ \mu \left( \frac{\partial u_i}{\partial x_j} + \frac{\partial u_j}{\partial x_i} \right) \right] + \frac{\partial}{\partial x_j} (-\overline{\rho u_i' u_j'}) + f_i \quad (5)$$

where the term  $\overline{\rho u_i' u_j'}$  represents the Reynolds stresses in turbulent flow, which is an indication of the velocity fluctuations from the average value.

$$-\overline{\rho u_i' u_j'} = 2\mu_t S_{ij} - \frac{2}{3} \delta_{ij} \frac{\partial u_k}{\partial x_k} - \frac{2}{3} \rho k \delta_{ij} \quad (6)$$

where  $\mu_t$  is the turbulent viscosity and Eddy viscosity models are used for the simulation and calculation of this parameter. The k- $\epsilon$  Realizable turbulent model has been used due to the high pressure gradients in the system.

$$\frac{\partial}{\partial t} (\rho k) + \frac{\partial}{\partial x_j} (\rho k u_j) = \frac{\partial}{\partial x_j} \left[ \left( \mu + \frac{\mu_t}{\sigma_k} \right) \frac{\partial k}{\partial x_j} \right] + G_k + G_b - \rho \epsilon - Y_M \quad (7)$$

$$\frac{\partial}{\partial t} (\rho \epsilon) + \frac{\partial}{\partial x_j} (\rho \epsilon u_j) = \frac{\partial}{\partial x_j} \left[ \left( \mu + \frac{\mu_t}{\sigma_\epsilon} \right) \frac{\partial \epsilon}{\partial x_j} \right] + \rho C_1 S \epsilon - \rho C_2 \frac{\epsilon^2}{k + \sqrt{\nu \epsilon}} + C_{1\epsilon} \frac{\epsilon}{k} C_3 G_b \quad (8)$$

where

$$C_1 = \max \left[ 0.43, \frac{\eta}{\eta + 5} \right], \eta = S \frac{k}{\epsilon}, S = \sqrt{2 S_{ij} S_{ij}} \quad (9)$$

$$\mu_t = \rho C_\mu \frac{k^2}{\epsilon}, C_\mu = \frac{1}{A_0 + A_S \frac{k U^*}{\epsilon}} \quad (10)$$

$$U^* = \sqrt{S_{ij} S_{ij}}$$

The constants of the equations are defined and calculated as follows:

$$A_0 = 4.04, A_S = \sqrt{6} * \cos \phi \quad (11)$$

$$\phi = \frac{1}{3} \cos^{-1}(\sqrt{6}W), W = \frac{S_{ij} S_{jk} S_{ik}}{\tilde{S}^3}, \tilde{S} = \sqrt{S_{ij} S_{ij}}, S_{ij} = \frac{1}{2} \left( \frac{\partial u_i}{\partial x_j} + \frac{\partial u_j}{\partial x_i} \right) \quad (12)$$

$$C_{1\epsilon} = 1.44, C_2 = 1.9, C_3 = 0.8, \sigma_k = 1.0, \sigma_\epsilon = 1.2$$

### 3.1. Grid generation

In computational fluid dynamics (CFD), several computational grids are used to generate the computational domain. These grid meshes include structured and unstructured ones. Due to the complexity of the geometry discussed in this study, an adaptive mesh is used. To create the adaptive mesh, at first, a primary mesh based on the geometry is

created. Then the grid becomes smaller by solving the equations on the grid, in areas where different gradients flow. Choosing the benchmark for grid matching is important. In this research, pyramid elements are used in grid generation. Using the adaptive mesh and generation of elements in high gradient regions, each element has become four pyramidal elements which lead to the increase in the number of elements and the increase in

the accuracy of the solution. For instance, in Model II, at an angle of  $45^\circ$ , air flow rate of 20 m/s, with initial 800,000 elements, after several times using the adaptive mesh, the number of elements is increased to 2100,000 which results in the increase in the accuracy of numerical simulation.

In order to evaluate the hydrodynamic behaviour of a four-sided wind tower, a geometrical representation of the wind tunnel testing set-up is produced numerically. The simulation is carried out in the range of  $0^\circ$  for a uniform wind velocity of 20 m/s. According to Fig. 8, the entrance boundary condition is inlet velocity and the exit boundary condition is outlet pressure. Because of the symmetric geometry of wind tower and bottom space, the boundary conditions of the symmetric surfaces of the wind tower and the bottom of residential space are symmetric.

#### 4. Results and Discussion

Comparing numerical results with experimental results helps us to analyse laboratory instrument and approaches. Also,

numerical simulation estimates the optimum places for inserting the total and the static pressure tubes, and makes it possible to calculate the flow rate and the velocity, which are the most important parameters of this study. The results obtained from the experimental and the numerical methods through Model I and Model II at various angles are shown in Table. 2. The relative confirmation between the numerical and the laboratory results in the wind tunnel shows the correctness of the tests.

Figure 9 shows the flow regime around Model I and Model II in the test chest and in the bottom chest (room) for a velocity of 20 m/s and an angle of attack of  $0^\circ$ . It can be clearly seen in the internal trap and close to the internal edge that a whirlpool and a flow separation have occurred, which led to the reduction of wind tower capacity. Also, Fig. 9 shows the flow separation and pressure reduction at the bottom, which is the main reason for air suction into the wind tower.

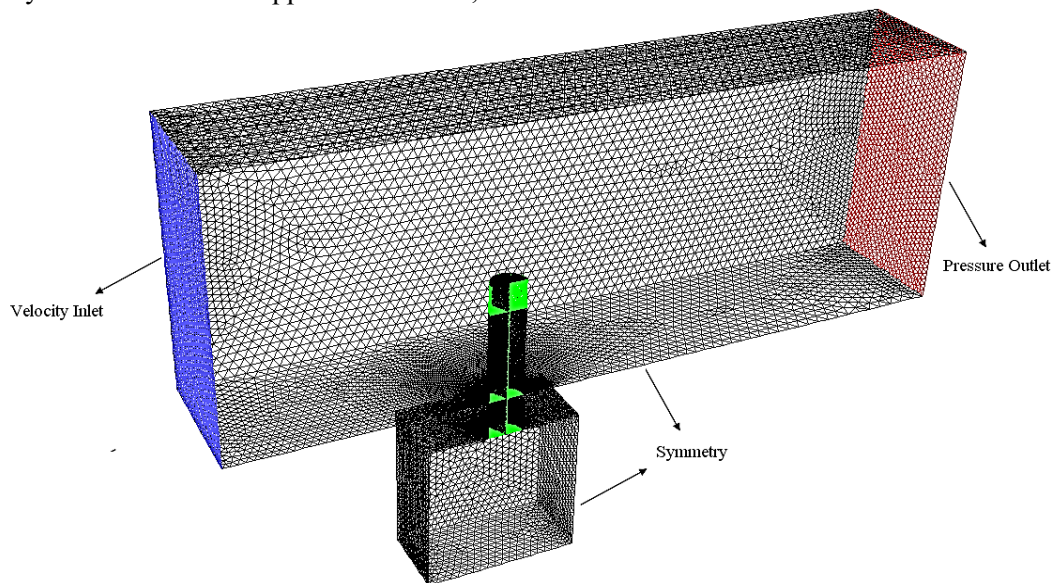


Fig. 8. Meshing of the simulated wind tunnel, wind tower and test room along the boundary.

Table 2. Volumetric airflow through the different channels of Model II for different air incident angles

Wind angle	A		B		C		D		Supply segments	
	EXP.	Numerical	EXP.	Numerical	EXP.	Numerical	EXP.	Numerical	EXP.	Numerical
0	0.0207	0.0197	0.0090	0.0078	0.0050	0.0036	0.000	0.0000	0.0207	0.0193
15	0.0203	0.0197	0.0094	0.0098	0.0092	0.0082	0.0013	0.0017	0.0217	0.0214
30	0.0186	0.0153	0.0122	0.0129	0.0127	0.0115	0.0076	0.0091	0.0263	0.0263
45	0.0143	0.0121	0.0125	0.0122	0.0132	0.0120	0.0143	0.0121	0.0287	0.0242



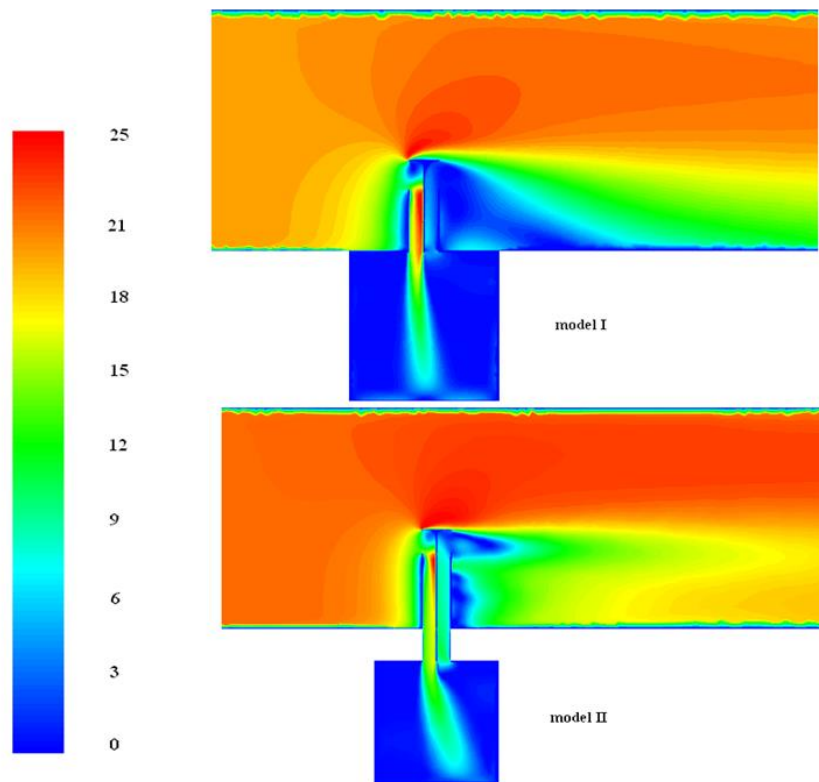


Fig. 9. Flow regime around Model I and Model II.

Figure 10 shows the path lines at  $0^\circ$  angle of attack for Model I, and at angles of attack of  $0^\circ$ ,  $15^\circ$ ,  $30^\circ$  and  $45^\circ$  for Model II. In addition, the resultant whirlpool at the back of the wind tower implies negative pressure area which leads to inducted air suction from other traps after crossing from the bottom space. These path lines show air entering into the bottom of Model I and  $0^\circ$  angle of attack without short-circuiting at  $15^\circ$  angle of attack which increases in the presence of little short-circuiting and at  $30^\circ$  and  $45^\circ$  angles.

Figure 11 shows the natural ventilation efficiency of Model I and Model II. It is obvious that the maximum efficiency of Model I occurs at  $45^\circ$  and the minimum efficiency occurs at  $10^\circ$  with a difference of 37%. As for Model II, the maximum efficiency occurs at  $45^\circ$  and it is minimum at  $0^\circ$  with a difference of 38%. It is observed that all models have the same volume, face surface and geometry, but the sectional surface of Model I is a circle quarter and that of Model II is a triangle. Therefore, it would be possible to compare them to find the optimum model.

Figure 12 shows the velocity distribution at the bottom and the top of all the three channels

of the wind tower channels II. These figures show the sensitive influence of static and total pressure at the channel section, which play an important role on laboratory error. For this purpose, laboratory errors could be reduced by inserting several tubes.

Now by creating turbulence in this model trap, the aim is to increase the model efficiency. Comparison between the different turbulence states is shown in Fig. 13, in which A, B, C, D, E, F show the vertical blade, horizontal blade, crown at bottom, crown at top, crown at bottom and top, and without turbulence, respectively. It is obvious from this figure that the wind tower performance is increased more by inserting vertical blade than horizontal blade. Also, inserting crown at the top of the wind tower promotes wind tower performance more than inserting crown at the bottom of the wind tower. Figure 14 shows the comparison between the supplied airflow for Model I and Model II. It is evident from this figure that at all angles, Model II shows better performance. In this study, the air attack velocity and the measuring methods were the same as in the study by Montazeri [20]. The Montazeri model is a 4-sided cylindrical wind tower with the difference of inserting a window at the bottom space. So a

comparison can be performed on wind tower samples. The quantity of airflow at different angles of attack is shown in Fig. 15. It is clear from Fig. 15 that Model II with triangular section has a better performance at the same

angle than Model I and Montazeri's cylindrical model, and this could be attributed to the existence of sharp edges. Sharp edges lead to a great separation area and more pressure difference at the width of the wind tower.

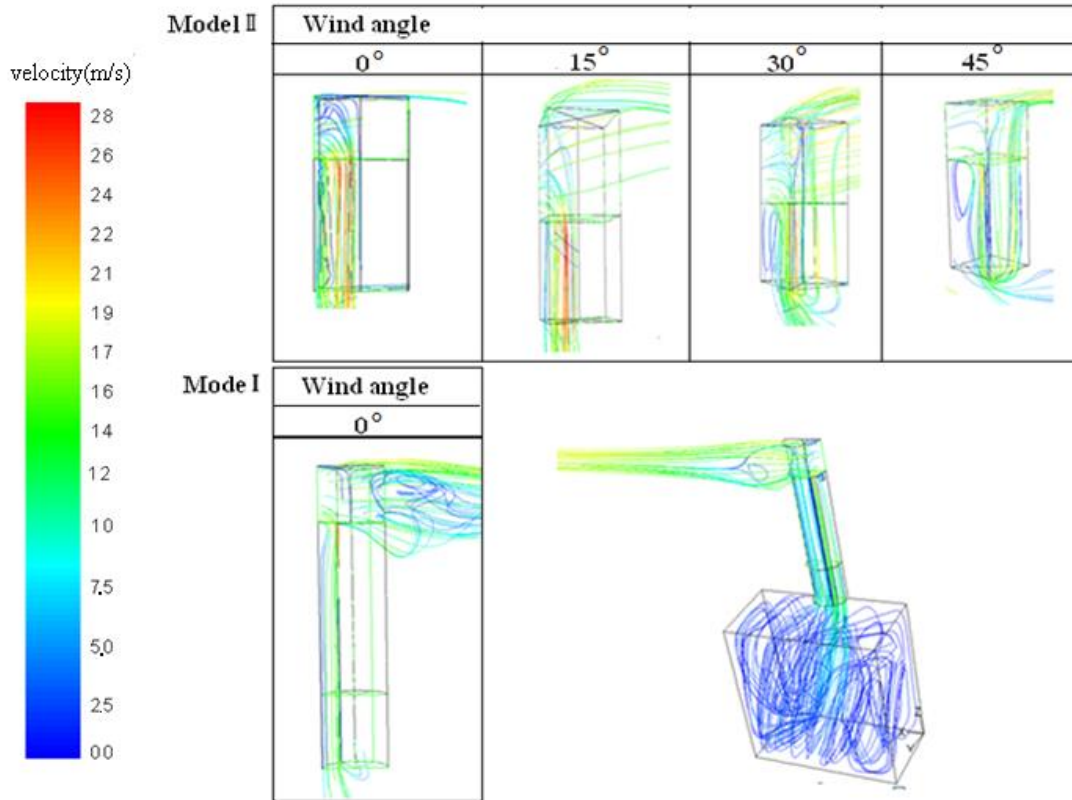


Fig. 10. Path lines at 0° angle of attack for Model I and at angles of attack of 0°, 15°, 30°, 45° for Model II.

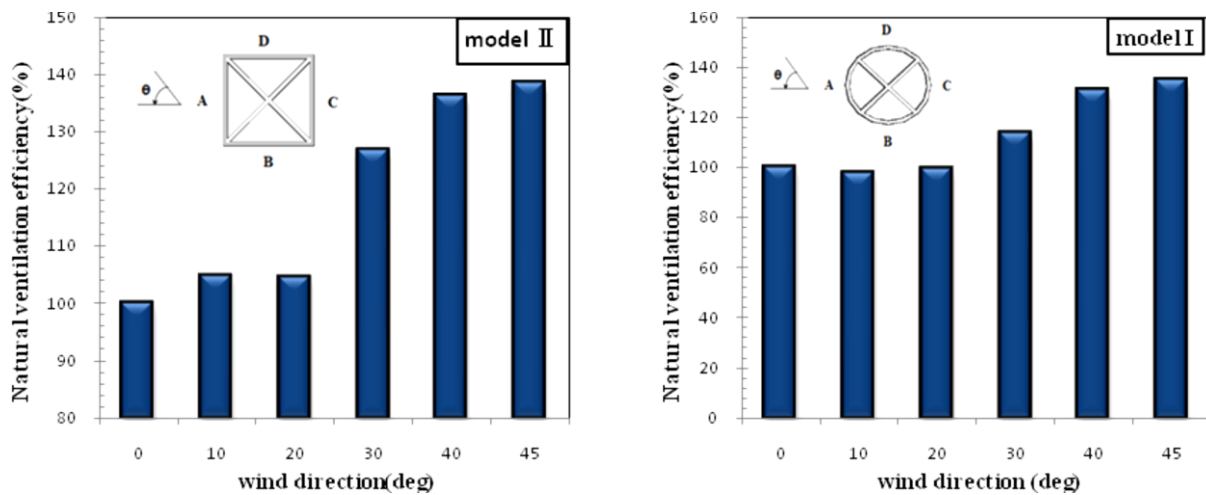


Fig. 11. The natural ventilation efficiency of Model I and Model II.

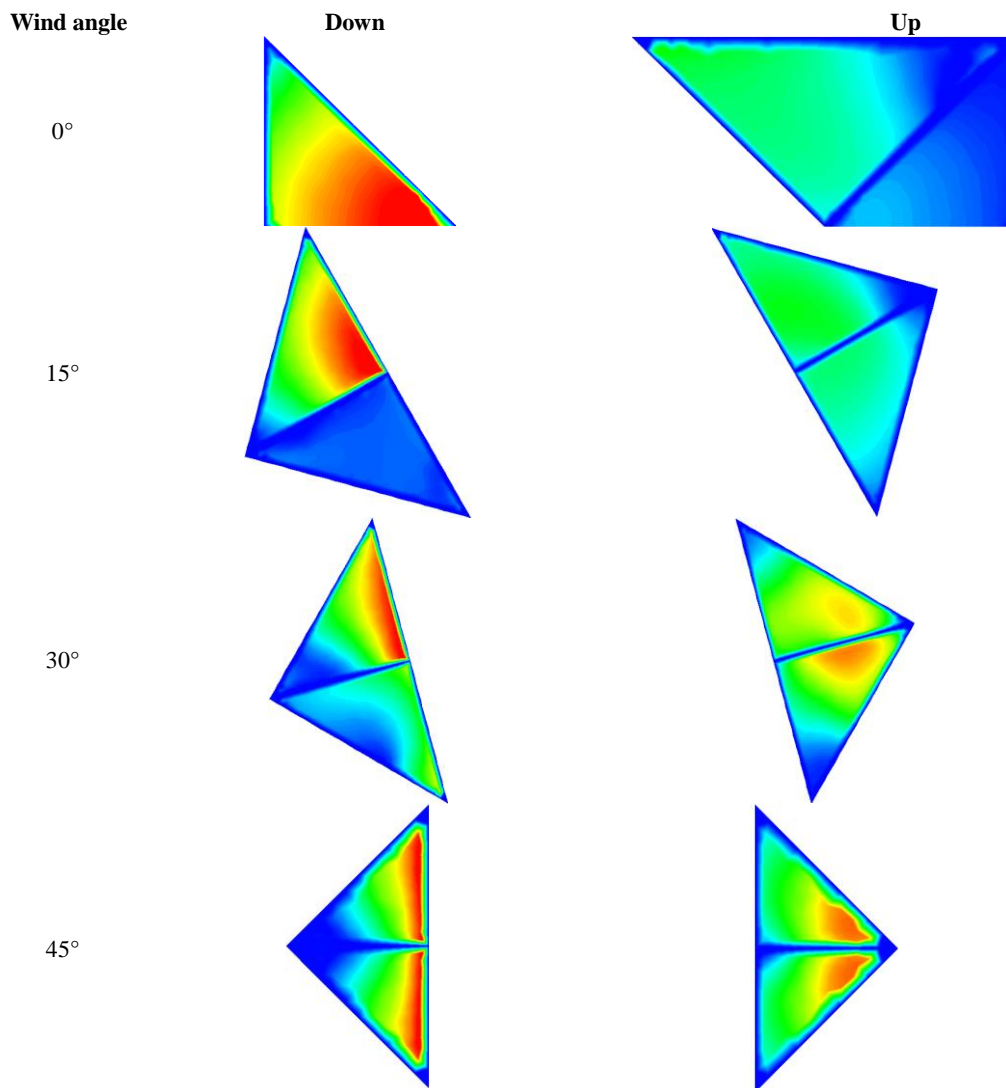


Fig. 12. Numerical results of the air velocity distribution at the bottom and the top of all three channels of the wind tower channels II.

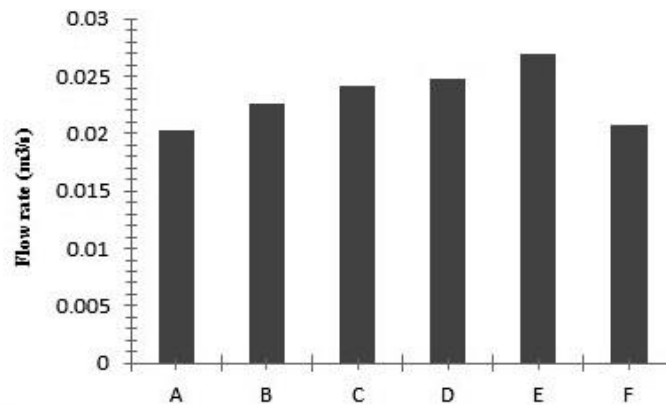


Fig. 13. Comparison between different turbulence states: (A) vertical blade, (B) horizontal blade, (C) crown at bottom, (D) crown at top, (E) crown at bottom and top, and (F) without turbulence.

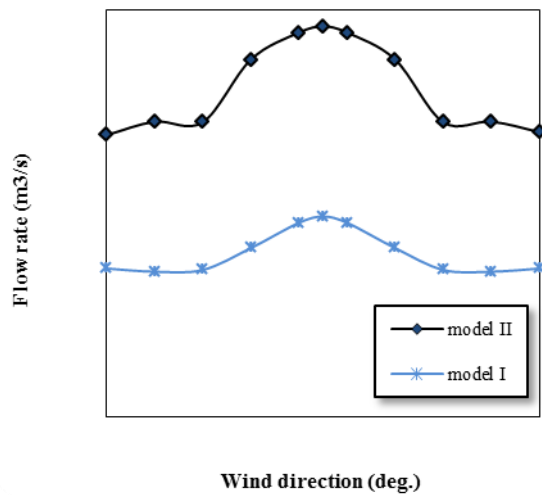


Fig. 14. Comparison between the supplied air flow for Model I and Model II.

## 5. Conclusion

In the present study, the evaluation of the influence of two symmetric 4-sided wind towers at flow induction to the bottom space in wind tunnel was performed using laboratory studies. At this state, the different models of 4-sided wind tower were installed at a laboratory wind tunnel and the air flow rate from every channel was measured to evaluate the wind tower induction performance at different wind blowing angles. In order to compare as well as to be assured of the applied methods, numerical simulation was performed by computational fluid dynamics, which showed relative agreement with the laboratory study. As evident from Table 2, the suction of traps leads to an increase in efficiency at all degrees except at  $0^\circ$ . Moreover, the results show that flow separation at the bottom area from the internal edge is one of the reasons for reduced flow induction to the bottom space. This flow separation and whirlpool in Model II, which has triangular section, is less than the other model, which has a quarter circular section. So, it can be concluded that sharp edges are one of the reasons for whirlpool reduction and they create an extended area of flow separation and more pressure difference at the wind tower's width, which lead to more flow induction. Inserting horizontal blades and crown at the top of the model, crown at the bottom and at the top, and bottom lead to an increased flow rate of 8, 16, 14, and 23%, respectively. The results showed the whirlpool reduction at the

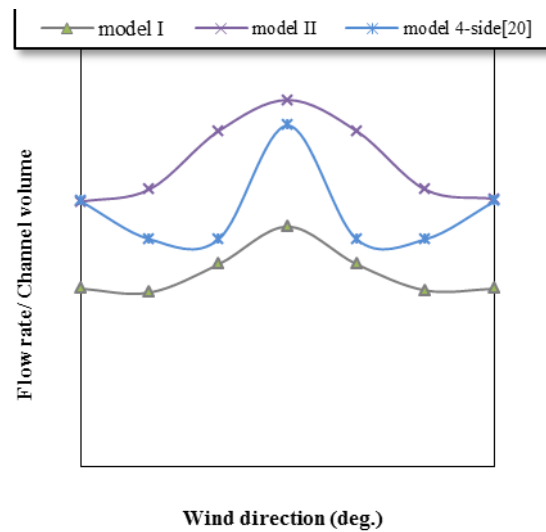


Fig. 15. The net ventilated air flow per channel volume of the wind tower for different models.

internal section of the channel and the increase in pressure coefficient. Moreover, installing vertical blades did not have an effect on flow induction. The quantity of flow induction to the house depends on the pressure coefficients inside and outside the channels. These coefficients vary according to the variation of the angle of attack. In Model I, the maximum ventilation efficiency occurred at an angle of  $45^\circ$  and the minimum occurred at  $10^\circ$  with a difference of 37%, and the maximum natural ventilation efficiency of Model II occurred at  $45^\circ$  and the minimum occurred at  $0^\circ$  with a difference of 38%.

## References

- [1] Battle G.S., Zanchetta M., Heath P., Wind Towers and Wind Driven Ventilation, The Energy for the 21st Century World Renewable Energy Congress VI (2000) 432-437.
- [2] Montazeri H., Azizian R., Experimental Study on Natural Ventilation Performance of a Two-Sided Wind Catcher, Journal of Power and Energy (2008) 223: 387-400.
- [3] Yuehong Su., Riffat S.B., Lin Y., Khan N., Experimental and CFD Study of Ventilation Flow Rate of a Monodraught(TM) Windcatcher, Energy and Buildings (2008) 40(6): 1110-1116.
- [4] Fathy H., Natural Energy and Vernacular Architecture: Principles and Examples with Reference to Hot Arid Climates (1986)

- ISBN-10: 0226239179, The University of Chicago Press.
- [5] Gage S.A., Graham J.M.R., Static Split Duct Roof Ventilation, *Building Research & Information* (2010) 28(4): 234–44.
- [6] Elmualim A.A., Smith S., Riffat S.B., Shao L., Evaluation of Dichroic Material for Enhancing Light Pipe/natural Ventilation and Daylighting in an Integrated System, *Applied Energy* (1999) 62(4): 253–266.
- [7] Bahadori M.N., Viability of Wind Towers in Achieving Summer Comfort in the Hot Arid Regions of the Middle East, *Renewable Energy* (1994) 5(5–8): 879–892.
- [8] Bansal N. K., Mathur R., Bhandari M. S., A Study of Solar Chimney Assisted Wind Tower System for Natural Ventilation in Buildings, *Building and Environment* (1994) 29(4): 495–500.
- [9] Liu L., Mak C.M., The Assessment of the Performance of a Windcatcher System Using Computational Fluid Dynamics, *Building and Environment* (2007) 42(3): 1135–1141.
- [10] Montazeri H., Azizian R., Experimental Study on Natural Ventilation Performance of One-Sided Wind Catcher, *Building and Environment* (2008) 43(12): 2193–2202.
- [11] Harris D.J., Webb R.S., Wind Towers Old Technology to Solve a New Problem, 17th AIVC Conference of Optimum Ventilation and Air Flow Control in Buildings, Gothenburg, Sweden (1996) 613–621.
- [12] Yaghoubi M.A., Sabzevari A., Golneshan A.A., Wind Towers: Measurement and Performance, *Solar Energy* (1991) 47(2): 97–106.
- [13] Bahadori M.N., Pressure Coefficients to Evaluate Air Flow Pattern in Wind Towers, *Proceedings of the International Passive and Hybrid Cooling Conference*, Miami Beach, FL: American Section of ISES (1981) 206–210.
- [14] Karakatsanis C., Bahadori M.N., Vickery B.J., Evaluation of Pressure Coefficients and Estimation of Air Flow Rates in Buildings Employing, Wind Towers Solar Energy (1986) 37(5): 363–374.
- [15] Elmualim A.A., Hazim B.A., Wind Tunnel and CFD Investigation of the Performance of Windcatcher Ventilation Systems, *International Journal of Ventilation* (2002) 1(1): 53–64.
- [16] Montazeri H, Dehghan A.A., Numerical Investigation of Induced Air Inside a Typical Building Through a Wind Catcher as a Passive Cooling Component, 13th Fluid Dynamics Conferences Yazd Iran (2006).
- [17] Elmualim A.A., Verification of Design Calculations of a Wind Catcher/Tower Natural Ventilation System with Performance Testing in a Real Building, *International Journal of Ventilation* (2006) 4(4): 393–404.
- [18] Montazeri H., Montazeri F., Azizian R., Mostafavi S., Two-Sided Wind Catcher Performance Evaluation Using Experimental, Numerical and Analytical Modeling, *Renewable Energy* (2010) 35(7): 1424–1435.
- [19] Elmualim A.A., Effect of Damper and Heat Source on Wind Catcher Natural Ventilation Performance, *Energy and Buildings* (2006) 38(8): 939–948.
- [20] Montazeri H., Experimental and Numerical Study on Natural Ventilation Performance of Various Multi-Opening Wind Catchers, *Building and Environment* (2011) 46(2): 370–378.